Scientific Reports

https://doi.org/10.1038/s41598-025-34689-7

Article in Press

Activation of M1mAChR's improves spatial learning and memory deficits in rats exposed to chronic intermittent hypoxia

Received: 31 March 2025

Accepted: 30 December 2025

Published online: 13 February 2026

Cite this article as: Huang Q., Hu C., Liu H. *et al.* Activation of M1mAChR's improves spatial learning and memory deficits in rats exposed to chronic intermittent hypoxia. *Sci Rep* (2026). https://doi.org/10.1038/s41598-025-34689-7

Qin Huang, Ci Hu, Haijun Liu, Chunfei Liu, Xiaodong Liu, Zucai Xu & Ping Xu

Activation of M1mAChR's Improves Spatial Learning and Memory Deficits in Rats Exposed to Chronic Intermittent Hypoxia

Qin Huang [1,2], Ci Hu[1], Haijun Liu[1,2], Chunfei Liu[1], Xiaodong Liu[1], Zucai Xu[1,2], Ping Xu[1]

[1]Department of Neurology, Affiliated Hospital of Zunyi Medical University 149 Dalian Road, Zunyi, Guizhou 563003, China

[2]Key Laboratory of Brain and Function and Brain Disease Prevention and Treatment of Guizhou Province

Correspondence:

Zucai Xu

Department of Neurology, Affiliated Hospital of Zunyi Medical University

149 Dalian Road, Zunyi, Guizhou, China, 563003

Email: docxzc@126.com

Ping Xu

Department of Neurology, Affiliated Hospital of Zunyi Medical University

149 Dalian Road, Zunyi, Guizhou, China, 563003

Email: xuping@zmu.edu.cn

Both Zucai Xu and Ping Xu are Corresponding Author

Abstract

Background: Obstructive sleep apnea (OSA) is characterized by chronic intermittent hypoxia (CIH), which drives neurodegeneration through oxidative and inflammatory stress and heightened synaptic vulnerability. However, the molecular circuitry linking CIH to hippocampal dysfunction remains incompletely defined.

Methods: In this study, Sprague–Dawley rats were exposed to CIH for 28 consecutive days, achieved by repeated hypoxia–reoxygenation cycles in a normobaric chamber. Hematoxylin–eosin (HE) staining was used to assess hippocampal histopathology. Hippocampal protein abundance of total STAT3 (t-

STAT3), phosphorylated STAT3 (p-STAT3), and the M1mAChR was quantified by immunoblotting. Immunohistochemistry was performed to determine the regional and cellular localization of t-STAT3, p-STAT3, and M1mAChR within the hippocampus.

Results: The present study demonstrated that exposure to CIH produces marked hippocampal-dependent spatial learning and memory deficits, together with reduced hippocampal neuronal density and lower expression of the M1mAChR and STAT3. Notably, AG490, a selective JAK2 inhibitor, did not improve behavioral performance in CIH-exposed rats. By contrast, the selective M1mAChR agonist VU0364572 partially rescued the CIH-induced deficits, consistent with a neuroprotective role for M1mAChR activation in CIH-related dysfunction.

Conclusion: Taken together, CIH induces hippocampal-dependent spatial learning and memory deficits accompanied by downregulation of hippocampal STAT3 and M1mAChR. The selective M1mAChR agonist VU0364572 partially reversed these deficits; however, this benefit required intact JAK2/STAT3 signaling (abolished by AG490). These findings support functional crosstalk between M1mAChR and JAK2/STAT3 in CIH-related hippocampal dysfunction, thereby contributing to improved learning and memory in rats.

Key words: Obstructive sleep apnea syndrome, Chronic intermittent hypoxia, M1mAChR, Janus kinase 2/signal transducer and activator of transcription 3

Highlights

CIH impairs hippocampal-dependent spatial learning and memory in rats.

CIH is associated with reduced hippocampal STAT3 and M1mAChR expression.

The selective M1 agonist VU0364572 partially rescues CIH-induced deficits.

1 | INTRODUCTION

OSAS is a common sleep-disordered breathing condition marked by recurrent upper-airway collapse during sleep[(1)]. Nocturnal sleep modulates brain activity and preserves structural integrity through multiple interacting complex mechanisms. Substantial evidence indicates that OSAS adversely affects cognition—most notably

attention, vigilance, memory, visuospatial abilities, and executive function—although the precise mechanisms remain incompletely defined[2].A growing body of evidence indicates that OSAS is associated with cognitive impairment—particularly in attention, vigilance, memory, visuospatial processing, and executive function—although the underlying mechanisms remain incompletely defined[3]. As a central pathophysiological hallmark of OSAS, CIH—recurrent hypoxia–reoxygenation exposure—elicits heightened oxidative stress, systemic inflammation, endothelial dysfunction, and sympathetic overactivation, thereby contributing to excessive daytime sleepiness, memory decline, and executive dysfunction[4, 5]. Experimental and neuroimaging studies have linked intermittent hypoxia (IH) to reduced neuronal density and altered neuronal signaling within the hippocampus and frontal cortex. [6, 7].

The JAK2/STAT3 signaling axis is a critical mediator of diverse physiological and pathological processes and has garnered increasing attention in obstructive sleep apnea (OSA) research. It participates in cell proliferation, differentiation, immune regulation, and apoptosis, and is notably active in neural tissue[8, 9], JAKs are non-receptor tyrosine kinases activated downstream of cytokine and growth-factor receptors; upon activation, JAK2 phosphorylates STAT3 (Tyr705), promoting STAT3 dimerization, nuclear translocation, and transcriptional regulation of target genes[10]. Once activated, JAK2 phosphorylates STAT3 at Tyr705, triggering STAT3 dimerization, nuclear translocation, and transcriptional regulation of target genes[11]. Recent studies suggest crosstalk between JAK2/STAT3 signaling and the M1mAChR, a key modulator of hippocampal plasticity and memory. Acetylcholine, acting predominantly through M1 receptors in the cortex and hippocampus, is indispensable for learning and memory and supports normal cognitive function[12] . Damage to cholinergic neurons or disruption of postsynaptic acetylcholine receptor signaling has been linked to cognitive deficits across multiple neuropsychiatric disorders, including Alzheimer's disease（AD）[13] and schizophrenia [14]. MAChRs are G protein–

coupled receptors (GPCRs) comprising five subtypes (M1–M5) distinguished by their G-protein coupling and downstream signaling. Among these, the M1 subtype (M1mAChR) is most abundant in the cerebral cortex and hippocampus. Genetic ablation of M1mAChR in mice produces pronounced memory deficits. In addition, elevating acetylcholine levels increases pyramidal-cell excitability[15], and selective M1 agonists enhance hippocampal synaptic plasticity, in part by potentiating N-methyl-D-aspartate receptor (NMDAR) signaling [16]. Prior studies indicate that pharmacological activation of M1mAChRs can alleviate cognitive deficits in mouse models of AD mice[13]. Moreover, Chiba et al. suggested that JAK2/STAT3 activation may upregulate cell-surface M1 mAChR and augment NMDAR-dependent LTP, which could contribute to improved cognitive performance in AD mouse models [17].

To investigate this relationship, we established a rat model of CIH to recapitulate key pathophysiological features of OSAS. We then employed two pharmacological probes: AG490, a selective JAK2 inhibitor, and VU0364572, a selective M1mAChR agonist. By integrating behavioral assays with quantification of hippocampal STAT3 and M1mAChRexpression, this study delineates their contribution to CIH-induced hippocampal-dependent spatial learning and memory deficits. The findings are expected to provide novel mechanistic insights and identify potential molecular targets for the prevention and treatment of OSAS-associated neurocognitive dysfunction.

2 | Materials and methods

2.1 | Animals and Grouping

Specific-pathogen-free (SPF) grade healthy adult male SD rats, weighing 150–180 g, were used in this study. The animals were obtained from the Experimental Animal Center of the Third Military Medical University (License No. SCXK 2012-0005, Chongqing, China). Rats were housed individually in a temperature-controlled room

(22–24 °C) on a 12:12 h light–dark cycle with ad libitum access to food and water. Animals were acclimated for 7 days before experimentation. At study completion, all rats were euthanized in accordance with institutional and national ethical guidelines to minimize suffering. All animal procedures conformed to institutional guidelines and were approved by the Animal Ethics Committee of Zunyi Medical University (approval No. [2020]1-318). This study complied with the ARRIVE guidelines (https://arriveguidelines.org) for reporting animal research. All efforts were made to minimize the number of animals used and to alleviate suffering. At the end of the study, rats were euthanized by intraperitoneal injection of sodium pentobarbital (3%, 50 mg/kg), in accordance with institutional and national guidelines.

2.2 | Establishment of CIH model and drugs treatments

54 rats were randomly assigned to six groups: control (CON), CIH, AG490 pretreatment, VU0364572 pretreatment, AG490 + VU0364572 combined pretreatment, and dimethyl sulfoxide (DMSO) vehicle control. The CIH paradigm was established according to published protocols with minor modifications[18]. Rats were subjected to intermittent hypoxia in a normobaric chamber 8 h/day for 28 days. Oxygen concentration within the chamber was maintained at 8.0 ± 0.5% by controlled nitrogen infusion, and the hypoxia-normoxia cycle was repeated every 90 seconds. O_2 levels were continuously monitored and regulated by an automated controller.

For pharmacological interventions, rats in the treatment groups received intraperitoneal injections of the JAK2 inhibitor AG490 (4 mg/kg/day) and/or the M1mAChR agonist VU0364572 (0.1 mg/kg/day) 30 minutes prior to CIH exposure. The DMSO vehicle group was given an equivalent volume of 2% DMSO, whereas the CON group received normal saline and was maintained under normoxia. AG490 (Selleck, USA) and VU0364572 (Cayman, USA) were prepared as DMSO stocks (10 μM) and diluted immediately prior to injection to a final DMSO concentration of 0.1%.

2.3 | Morris water maze（MWM） behavioral tests

Spatial learning and memory performance were assessed using the Morris water maze (MWM) test, as previously described[19] . The protocol comprised acquisition (navigation) trials followed by a probe trial. Behavioral endpoints—escape latency during acquisition and platform-crossing frequency during the probe—were recorded and analyzed to quantify performance.

2.4 | Tissue preparation

At study termination, rats were deeply anesthetized with sodium pentobarbital (3%, 50 mg/kg, i.p.) prior to tissue collection. Organ harvest was performed in accordance with the approved Animal Care and Use Protocols of Zunyi Medical University. After confirming deep anesthesia, transcardial perfusion was performed using sterile 0.9% normal saline to clear the blood and preserve tissue morphology. Following perfusion, the brain was harvested. Hippocampal tissues or whole brains were collected and processed for subsequent histological and biochemical analyses.

2.5 | Western blotting

Hippocampal tissues were lysed, and total protein was extracted, quantified, and denatured. Equal amounts of protein were loaded onto SDS-PAGE gels, followed by electrophoresis and transfer onto PVDF membranes (IPVH00010, Millipore, USA) using a constant current of 250 mA for 110 minutes. After blocking, membranes were incubated overnight at 4°C with primary antibodies: total STAT3 (1:1000, #30835, CST, USA), p-STAT3 (p-STAT3; 1:1000, #9145, CST, USA), M1mAChR (1:500, #9808, Sigma, USA), and β-tubulin (1:1500, #10068, Proteintech, USA). The next day, membranes were incubated with HRP-conjugated secondary antibodies (1:5000, ZB-2305, ZSGB-BIO, China) at room temperature for 1 hour. Immunoreactive bands were visualized using enhanced chemiluminescence (ECL), and densitometric analysis was performed using ImageJ software.

2.5 | HE staining

Fixed brain tissues were embedded in paraffin and sectioned. The sections were deparaffinized, rehydrated through graded ethanol, and stained with hematoxylin and eosin. After dehydration and clearing, the sections were mounted using neutral resin. Histological changes in hippocampal tissue were observed and imaged using an inverted light microscope (Olympus, Tokyo, Japan).

2.6 | Immunochemistry

Paraffin-embedded brain sections (4μm) were prepared and processed using standard immunohistochemical protocols. After deparaffinization, antigen retrieval was performed in citrate buffer, followed by quenching of endogenous peroxidase activity with 3% H_2O_2 at 37°C for 15 minutes. Sections were blocked with goat serum and incubated overnight at 4°C with primary antibodies against STAT3 (1:50), p-STAT3 (1:50), and M1mAChR (1:40). The next day, slides were rewarmed at 37°C, incubated with an enhancer solution (Zhongshanjinqiao, China), followed by HRP-conjugated goat anti-rabbit IgG. Detection was carried out using DAB substrate, and counterstaining was performed with hematoxylin. After dehydration and clearing with ethanol and xylene, the slides were sealed with neutral resin and examined under a microscope (Olympus, Tokyo, Japan).

2.7| Statistical analysis

Data were analyzed using SPSS version 29.0 (IBM Corp., Armonk, NY, USA). Results are expressed as mean ± standard deviation (SD). Blood oxygen saturation measurements were analyzed using paired t-tests. MWM navigation data were assessed using repeated measures ANOVA. One-way ANOVA was used to compare data across multiple groups, followed by LSD post hoc tests for pairwise comparisons. A p-value of ≤ 0.05 was considered statistically significant.

3 | RESULTS

3.1 | Establishment of the CIH rat model

In this study, a rat model of OSAS was established by CIH. During the hypoxic phase, rats exhibited characteristic behavioral responses, including frequent arousals, upward head extension to facilitate breathing, and a marked increase in respiratory rate, accompanied by signs of agitation and restlessness. In contrast, during the reoxygenation phase, the animals demonstrated decreased locomotor activity, lethargy, and diminished responsiveness. To validate the CIH model, arterial oxygen saturation (SpO_2) in the rat tail was continuously monitored throughout hypoxia and reoxygenation cycles using a blood oxygen saturation detector. The mean SpO_2 ($MSpO_2$) during hypoxia was significantly reduced to 68.27 ± 2.43%, while it increased to 96.74 ± 1.58% during reoxygenation. The observed >4% decrease in oxygen saturation between hypoxia and reoxygenation phases was statistically significant ($p < 0.05$), confirming the successful induction of intermittent hypoxic conditions consistent with the pathophysiological features of OSAS. Collectively, the behavioral observations and oxygen saturation data indicate that the CIH model was effectively established and replicates the hallmark features of OSAS in rats （Table1）.

Table 1 Changes in rat tail SpO2 during hypoxia and reoxygenation in CIH model rats ($\bar{x}$±s)

Group	n	SpO2（%）
reoxygenation interval	45	96.74±1.58
Hypoxic interval	45	68.27±2.43▲

Note:▲Compared with the reoxygenation interval $p < 0.05$.

3.2 | Changes in MWM learning and memory of CIH rats.

The MWM was used to assess spatial learning and memory in CIH-exposed rats. (Figure 1). During the acquisition phase, the escape latency of all groups progressively decreased over the course of training, indicating the establishment of learning behavior. On the third day of training, rats in the VU0364572 group

exhibited escape latency comparable to that of the CON group ($p > 0.05$), while rats in the CIH, DMSO, AG490, and AG490 + VU0364572 groups demonstrated significantly prolonged escape latencies compared to the CON group ($p< 0.05$). Furthermore, compared to the VU0364572 group, escape latency was significantly longer in the DMSO, AG490, and AG490 + VU0364572 groups ($p< 0.05$), whereas no significant difference was observed between the CIH and DMSO groups ($p >0.05$). Twenty-four hours after the final training session, the hidden platform was removed, and a probe trial was conducted to evaluate spatial memory retention. In this test, rats in the CON group crossed the former platform location and time spent in the target quadrant significantly more times within 120 seconds compared to the CIH, DMSO, AG490, and AG490 + VU0364572 groups ($p < 0.05$). Similarly, the VU0364572 group exhibited a significantly higher number of platform crossings and time spent in the target quadrant than the CIH, DMSO, AG490, and AG490 + VU0364572 groups ($p < 0.05$), further confirming its cognitive-enhancing effect. Again, there was no statistically significant difference between the CIH and DMSO groups ($p > 0.05$). Collectively, these findings indicate that CIH induces substantial impairments in learning and memory in rats. Treatment with the JAK2 inhibitor AG490 exacerbates this cognitive dysfunction, while activation of the M1mAChR via VU0364572 markedly improves spatial learning and memory performance in CIH-exposed animals.

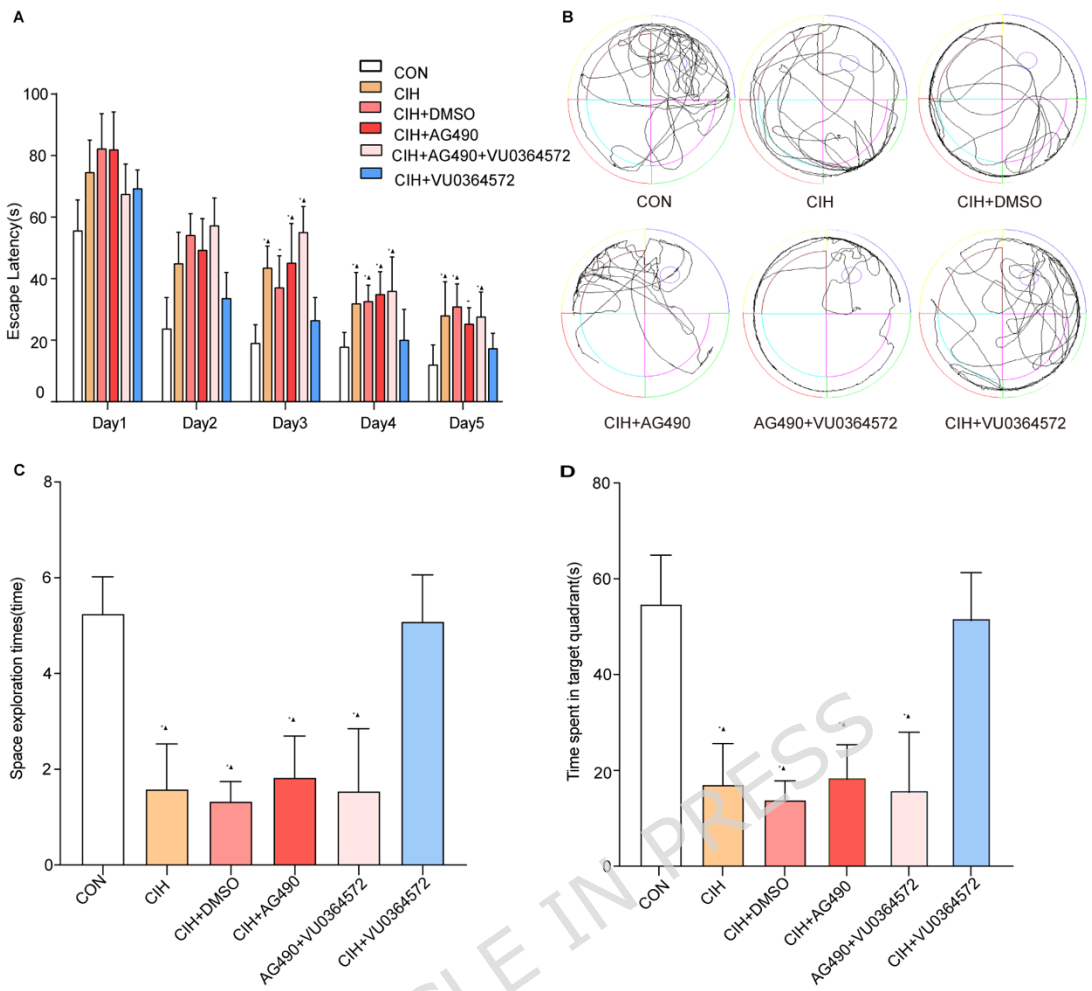

Figure1 Changes in MWM learning and memory of CIH rats in each group. (A) Changes in escape latencies in CIH model rats with AG490 or VU0364572 treatment. The CIH, DMSO, AG490, and AG490 + VU0364572 groups versus the CON group. The VU0364572 group compared with the CIH, DMSO, AG490, and AG490 + VU0364572. $F_{(5,150)}$ =33.17. All data are presented as mean ±SD (n = 6). Statistical analysis was performed by one-way ANOVA. *p <0.05, ▲p< 0.05. （B） Representative swimming trajectories illustrating search strategies in each group （day 6）. (C、D) Changes in the number of platforms crossing and time spent in the target quadrant in CIH model rats with AG490 or VU0364572 treatment (day6). The CIH, DMSO, AG490, and AG490 + VU0364572 groups versus the CON group. CIH, DMSO, AG490, and AG490 + VU0364572 group versus the VU0364572 group. All data are presented as mean ±SD (n = 6). Statistical analysis was performed by one-way ANOVA. *p <0.05, ▲p <0.05. (D) Changes in the number of platforms crossing

in CIH model rats with AG490 or VU0364572 treatment. The CIH, DMSO, AG490, and AG490 + VU0364572 groups versus the CON group. CIH, DMSO, AG490, and AG490 + VU0364572 group versus the VU0364572 group. $F_{(5.30)} = 24.62$. All data are presented as mean ±SD (n = 6). Statistical analysis was performed by one-way ANOVA. *$p < 0.05$, ▲$p < 0.05$.

3.3 | Histopathological Changes in the Hippocampus Revealed by HE Staining

HE staining was performed on hippocampal tissue samples collected from rats in the CON, CIH, DMSO, AG490, AG490 + VU0364572, and VU0364572 groups to assess morphological alterations in neuronal structure. In the CON group, hippocampal neurons were densely and orderly arranged, exhibiting well-defined cell bodies, intact nucleoplasm, and prominent nucleoli. In contrast, tissue sections from the CIH, DMSO, AG490, and AG490 + VU0364572 groups showed marked histopathological changes, including disorganized neuronal arrangement, blurred cellular boundaries, reduced neuronal density, and increased eosinophilic staining, indicative of neuronal degeneration. In some regions, neurons exhibited morphological features suggestive of necrosis. Statistical analysis confirmed a significant reduction in neuronal cell counts in these groups compared to the CON group ($p < 0.05$). Notably, the VU0364572-treated group exhibited attenuated histopathological damage, with more preserved neuronal architecture, higher cell density, and improved cellular organization relative to the CIH and AG490-treated groups. These findings suggest that CIH induces substantial hippocampal neuronal damage, while activation of M1mAChR with VU0364572 exerts a neuroprotective effect, mitigating CIH-induced neuronal loss and structural disruption in the hippocampus. (Figure2).

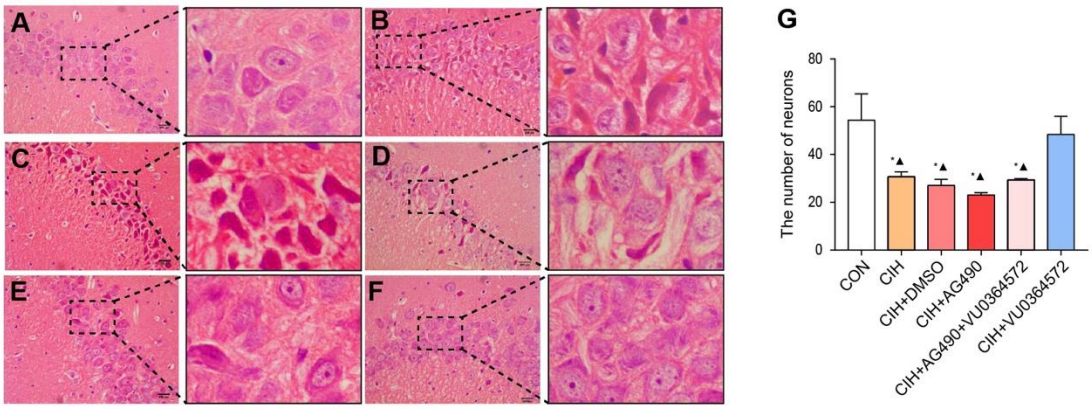

Figure 2 Observation of pathological changes in hippocampus of CIH rats (40 ×).

Note: the picture shows hippocampal neurons in each group of experimental rats. (A) CON group. (B)CIH group. (C) CIH+DMSO group. (D) CIH+AG490 group. (E) CIH+AG490 + VU0364572 group. (F) CIH+ VU0364572 group. (G) The CIH rat hippocampal CA1 area the number of neurons, *$p<0.05$, compared with the CON group, ▲$p<0.05$, compared with the VU0364572 group. All the data are expressed in mean ± SD.

3.4 | Western Blot Analysis of t-STAT3 and p-STAT3 Expression in the Hippocampus

Western blotting was employed to evaluate the expression levels of total STAT3 (t-STAT3) and phosphorylated STAT3 (p-STAT3) in the hippocampal tissues of rats from each experimental group. Densitometric analysis was performed using ImageJ software to quantify the integrated optical density (IOD) of the immunoreactive bands, and expression levels were normalized to β-tubulin. Compared to the CON group, the IOD ratios of p-STAT3/β-tubulin and t-STAT3/β-tubulin were significantly decreased in the CIH group ($p < 0.05$), indicating a reduction in both total and phosphorylated STAT3 protein expression following chronic intermittent hypoxia. Notably, the expression levels of p-STAT3 and t-STAT3 in the AG490, AG490 + VU0364572, and VU0364572 treatment groups showed no statistically significant difference compared to the CIH group ($p > 0.05$). Similarly, there was no

significant difference between the DMSO group and the CIH group for either p-STAT3 or t-STAT3 expression. Overall, these results suggest that CIH markedly suppresses STAT3 signaling activity in the hippocampus, as evidenced by the downregulation of both total and phosphorylated STAT3. Neither AG490 nor VU0364572 administration significantly restored STAT3 expression under CIH conditions, indicating that the observed cognitive and structural changes may involve STAT3-independent mechanisms or require additional regulatory factors. (Figure 3).

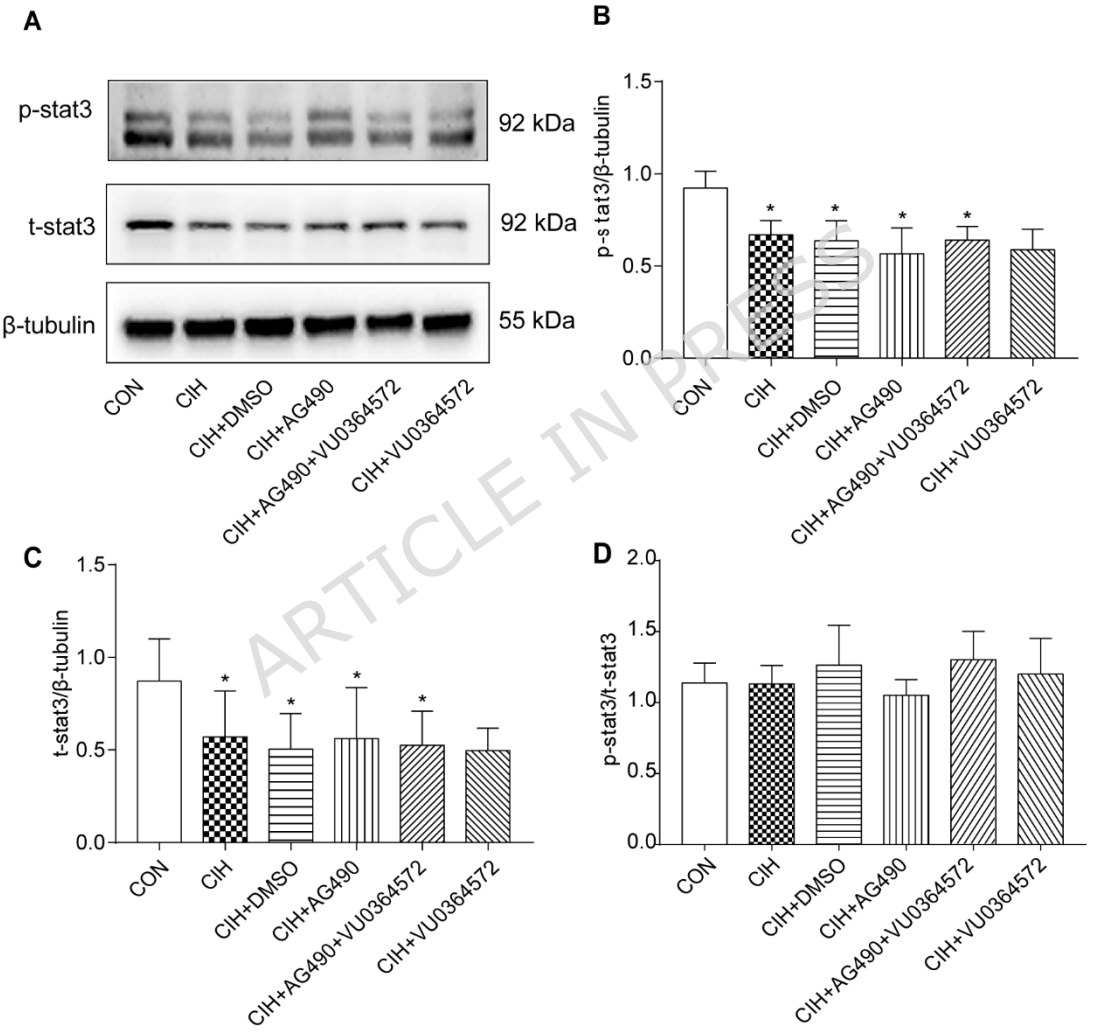

Figure 3 Changes of t-STAT3 and p-STAT3 protein expression in hippocampus of CIH rats. (A) Representative Western blots of p-STAT3，t-STAT3 proteins. (B) Relative p-STAT3 protein expression levels. (C) Relative t-STAT3 protein expression

levels. (D)Relative p-STAT3 /t-STAT3 protein expression levels. *$p<0.05$, compared with the CON group. All the data are expressed in mean ± SD.

3.5| Western Blot Analysis of M1mAChR Expression in the Hippocampus of CIH Rats

To evaluate alterations in M1mAChR expression in the hippocampus under CIH, Western blot analysis was performed, and band intensities were quantified using ImageJ software. The expression of M1mAChR was normalized to β-tubulin, and the IOD ratio (M1mAChR/β-tubulin) was calculated for each group. Compared to the CON group, the CIH group exhibited a significant reduction in M1mAChR expression ($p < 0.05$), indicating that CIH suppresses M1mAChR levels in hippocampal tissue. No statistically significant differences were observed between the CIH group and either the CIH+AG490 or CIH+AG490+VU0364572 groups ($p > 0.05$), suggesting that AG490, alone or in combination with VU0364572, did not effectively restore M1mAChR expression under CIH conditions. In contrast, the CIH+VU0364572 group showed a significant increase in M1mAChR expression compared to the CIH group ($p < 0.05$), highlighting the potential of M1mAChR agonist treatment in reversing CIH-induced receptor downregulation. Additionally, no significant differences were detected among the CIH+DMSO, CIH+AG490, and CIH+AG490+VU0364572 groups ($p > 0.05$). These findings suggest that activation of M1mAChR with VU0364572, but not inhibition of the JAK2/STAT3 pathway with AG490, effectively restores M1mAChR expression suppressed by CIH (Figure 4).

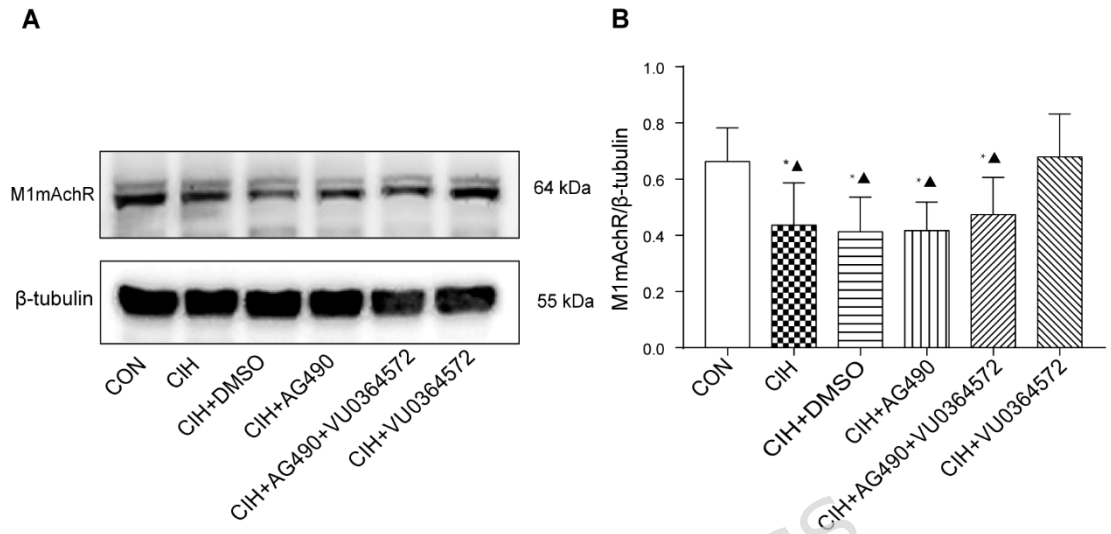

Figure 4 Changes of M1mAChR protein expression in hippocampus of CIH rats. (A) Representative Western blots of M1mAChR proteins. (B) Relative M1mAChR protein expression levels. *$p<0.05$, compared with the CON group, ▲$p<0.05$, compared with the VU0364572 group, all data are expressed in mean ± SD.

3.6 | Immunohistochemical Localization of t-STAT3 in the Hippocampus

Following the assessment of t-STAT3expression by Western blotting, immunohistochemical analysis was performed to determine the spatial distribution and cellular localization of t-STAT3 in the hippocampal CA1 region across different experimental groups. The results demonstrated positive immunoreactivity for t-STAT3, characterized by yellow to brown staining, predominantly localized in the CA1 subregion of the hippocampus. The protein was primarily expressed in the cytoplasm of hippocampal neurons, consistent with its known intracellular distribution pattern. These findings corroborate the Western blot results, confirming the presence and cytoplasmic localization of t-STAT3 in hippocampal neurons, and provide further insight into the regional expression patterns of t-STAT3 under CIH and treatment conditions. (Figure5).

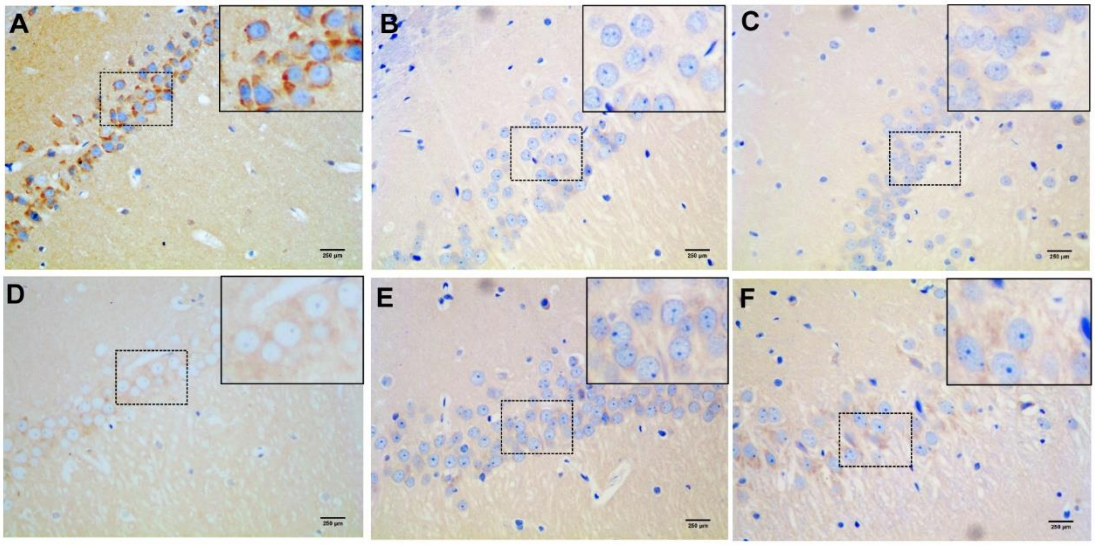

Figure 5 Immunohistochemical analysis of t-STAT3 in hippocampus of CIH rats (40 ×). (A) CON group. (B)CIH group. (C)CIH+DMSO group. (D)CIH+AG490 group. (E)CIH+ AG490+ VU0364572 group. (F)CIH+VU0364572 group. (scale = 250 μ m)

3.7| Immunohistochemical Localization of p-STAT3 in the Hippocampus

Following Western blot analysis of p-STAT3 expression across experimental groups, immunohistochemical staining was performed to further evaluate the distribution and localization of p-STAT3 within the CA1 region of the rat hippocampus. The results showed positive immunoreactivity for p-STAT3, characterized by yellow to brown staining predominantly observed in the cytoplasm of neurons located within the CA1 subregion. This spatial expression pattern was consistent across groups, providing morphological validation of the protein's presence and subcellular localization as identified by Western blotting. Together, these findings confirm that p-STAT3 is primarily localized in the cytoplasm of hippocampal neurons and support its potential involvement in CIH-related hippocampal signaling alterations(Figure6).

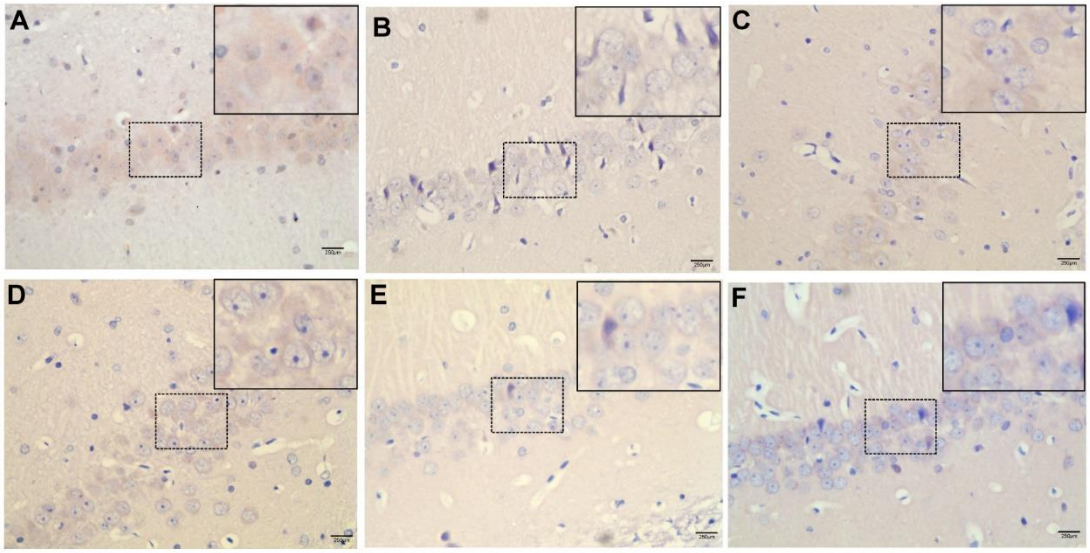

Figure 6 Immunohistochemical analysis of p-STAT3 in hippocampus of CIH rats (40 ×). (A)CON group. (B)CIH group. (C)CIH+DMSO group. (D)CIH+AG490 group. (E)CIH+ AG490+ VU0364572 group. (F)CIH+VU0364572 group. (scale = 250 μ m)

3.8 | Immunohistochemical Localization of M1mAChR in the Hippocampus

Immunohistochemical staining was performed to examine the expression pattern and localization of M1mAChR in the CA1 region of the hippocampus across experimental groups. The results demonstrated positive M1mAChR immunoreactivity, indicated by yellow to brown staining, predominantly localized in the CA1 subregion of the hippocampus. Notably, M1mAChR expression was primarily observed on the cell membranes of hippocampal neurons, consistent with its known role as a membrane-bound receptor (Figure 7). These findings provide morphological evidence of M1mAChR distribution in the hippocampus and support its potential involvement in CIH-related cognitive dysfunction and therapeutic modulation.

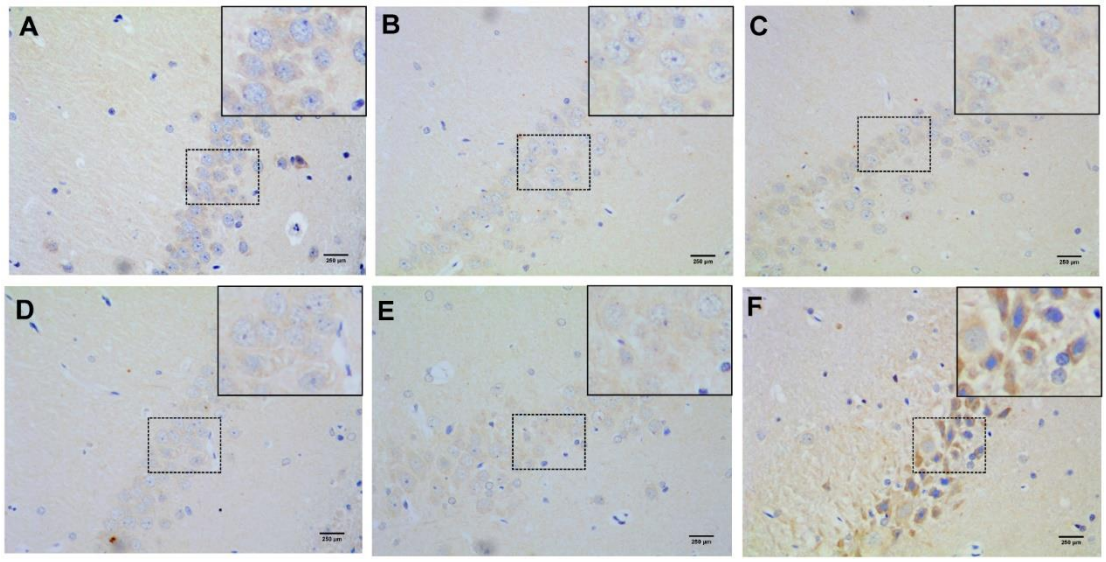

Figure 7 Immunohistochemical analysis of M1mAChR in hippocampus of CIH rats (40 ×). (A) CON group. (B)CIH group. (C)CIH+DMSO group. (D)CIH+AG490 group. (E)CIH+ AG490+ VU0364572 group. (F)CIH+VU0364572 group; (scale = 250 μ m)

4 | DISCUSSION

CIH, the core pathophysiological feature of OSAS, has been shown to induce neuronal loss in the hippocampus and frontal cortex, accompanied by disruptions in synaptic plasticity. Experimental evidence further suggests that CIH promotes oxidative stress, systemic inflammation, endothelial dysfunction, and sympathetic hyperactivation—factors that collectively impair neural function. Importantly, alterations in synaptic structure, quantity, and function are closely associated with the regulation of learning and memory and play a fundamental role in neuroplasticity.

In the present study, a CIH model was established to simulate the pathophysiological features of OSAS in rats. Repetitive cycles of hypoxia and reoxygenation were administered in a normobaric hypoxic chamber. Blood oxygen saturation monitoring confirmed a significant reduction during hypoxic episodes compared to reoxygenation phases (Figure 1). During hypoxic epochs, rats exhibited behavioral arousals, head-up posturing to facilitate breathing, and agitation. HE staining of the CA1 region revealed disorganized cytoarchitecture, nuclear pyknosis, widened intercellular

spaces, and reduced neuronal density in CIH-exposed rats relative to controls (Figure 2), consistent with successful model establishment.

Given the brain's sensitivity to oxygen availability, intermittent hypoxia exerts profound effects on cognitive functions such as learning, memory, and executive processing [20] [21]. MWM test, a well-established method for assessing spatial learning and memory in rodents[22], revealed that CIH-exposed rats showed significantly prolonged escape latencies relative to controls, consistent with impaired spatial learning and memory. Notably, pharmacological inhibition of JAK2/STAT3 with AG490 did not ameliorate these deficits. By contrast, pretreatment with VU0364572, a selective M1mAChR agonist, significantly shortened escape latency and improved performance toward control levels. These findings support a role for M1mAChR activation in modulating spatial learning and memory under CIH. This suggests that however, co-administration of AG490 and VU0364572 did not yield additive or synergistic behavioral benefits. We speculate that JAK2/STAT3 inhibition may abrogate signaling requisite for M1mAChR–mediated neuroprotection, thereby attenuating the behavioral efficacy of VU0364572 under CIH. Consistent with the acquisition data, the probe trial showed increased platform crossings only in the VU0364572-treated group, whereas AG490—alone or in combination—did not improve probe performance. These findings support a role for M1mAChR activation in mitigating CIH-related deficits in spatial learning and memory, whereas JAK2/STAT3 inhibition conferred no behavioral benefit and abrogated the M1-mediated improvement.

The JAK2/STAT3 pathway is known to mediate a wide range of cellular processes, including cell proliferation, differentiation, apoptosis, and inflammation[23, 24]. Its activation is triggered by cytokines, reactive oxygen species, and chemokines[25, 26]. STAT3 plays a versatile role in signal transduction and gene regulation. Upon JAK-dependent phosphorylation at the Tyr705 residue, STAT3 dimerizes and translocates to the nucleus, where it regulates transcription of genes implicated in neuronal

survival and synaptic plasticity[27-30]. Previous studies have shown that sustained hypoxia (24–48 h) alters STAT3 Tyr705 phosphorylation. We therefore focused on p-STAT3（Tyr705）as a key analytical endpoint[31].

Immunoblotting revealed robust hippocampal expression of t-STAT3 and p-STAT3) in controls, whereas CIH-exposed rats exhibited markedly reduced levels of both. This pattern is consistent with attenuated JAK2/STAT3 pathway activation in the hippocampus under CIH. Interestingly, administration of AG490, VU0364572, or the combination produced nominal increases in hippocampal t-STAT3 and p-STAT3, but these changes did not reach statistical significance relative to CIH controls, suggesting that M1mAChR stimulation may be insufficient to fully restore STAT3 signaling under CIH. As expected for a selective JAK2 inhibitor, AG490 suppressed STAT3 phosphorylation without significantly altering total STAT3 abundance in CIH-exposed hippocampi. These findings are consistent with prior reports of declines in learning and memory following intrathecal JAK2/STAT3 inhibition[32, 33]， and with result from Wang et al. who demonstrated that activating this pathway improves cognition in a cerebral small vessel disease model [34].The M1mAChR is a key modulator of cognition and has been proposed as a promising target for memory enhancement[35]. Park et al. reported that inhibition of JAK2/STAT3 may impair memory and contribute to cholinergic dysfunction[36]. Moreover, activation of the JAK2/STAT3 pathway has been shown to enhance spatial learning and memory [35].In parallel, the M1mAChR contributes to neuronal plasticity and cognitive regulation[37]. Prior research suggests that M1mAChR may exert its memory-enhancing effects, at least in part, through JAK2/STAT3 pathway activation.

In this study, the use of VU0364572, a specific M1mAChR agonist[38],led to improved learning and memory performance in CIH rats, confirming its therapeutic potential. However, when co-administered with AG490, the cognitive benefits were abolished, further indicating a functional interplay between M1mAChR activation and JAK2/STAT3 signaling. We therefore propose that M1mAChR activation can

partially mitigates CIH-related deficits in spatial learning and memory, with JAK2/STAT3 acting as a critical downstream mediator in this process. Our findings indicate that M1mAChR–dependent benefits under CIH require intact JAK2/STAT3 signaling, M1mAChR–driven benefits depend on intact JAK2/STAT3, but the direction of influence remains unresolved. Beyond JAK2/STAT3, M1mAChR likely confers CIH resilience via several convergent, pro-synaptic pathways， Gq/PLCβ–IP_3/Ca^{2+}–PKC and CaMKII/IV–ERK–CREB signaling enhance synaptic efficacy and drive plasticity genes, supporting dendritic spine stability[39, 40]. PI3K/Akt–mTOR sustains protein synthesis for long-term plasticity and may buffer CIH-related catabolic stress[41]; and Src-dependent NMDAR potentiation increases currents to facilitate LTP[42]. Additional crosstalk with survival programs (mitochondrial support, anti-apoptotic transcription) could further limit hypoxic injury. To test this framework, combine pathway-selective inhibitors and M1 antagonism with electrophysiological readouts NMDAR-LTP and molecular assays[43]. Integrated with the directionality experiments above, these studies will map how M1mAChR–JAK2/STAT3 interfaces with broader M1mAChR-coupled signaling to deliver synaptic and structural neuroprotection in CIH. We will test this in our subsequent experiments.

4 | CONCLUSION

In summary, CIH produced spatial learning and memory deficits, accompanied by reduced hippocampal neuronal density and downregulation of STAT3 and M1mAChR. Pharmacological activation of M1mAChRs with VU0364572 partially rescued these deficits, whereas JAK2 inhibition with AG490 conferred no benefit and abrogated the M1-mediated improvement.

Date availability statement

The datasets used and/or analyzed during the present study are available from the corresponding author on reasonable request.

Author contributions

QH and CH were responsible for overall supervision. QH and CH contributed to all experimental work. QJ contributed to data statistical analysis and written this article. HJ contributed to behavioral study design. XD and CF participated in biochemical parts of the experiment. FY drew these figures. ZC and PX designed this research. All the authors reviewed and approved the final manuscript.

Acknowledgements

This study was funded by the Young Scientific and Technological Talent Growth Project of Guizhou Provincial Department of Education (Grant No. Qianjiaoji [2024]145) and the Zunyi Municipal Science and Technology Support Program (Grant No. Zunshikehezhicheng [2025]41).

Competing interests

The authors declare that the research was conducted in the absence of any commercial or financial relationships that could be construed as a potential conflict of interest.

Conflict of interest statement

The authors declare no conflicts of interest. We also certify that the submission is original work and is not under review at any other publication.

References

1. Jordan AS, McSharry DG, Malhotra A. Adult obstructive sleep apnoea. Lancet. 2014;383(9918):736-47.

2. Olaithe M, Bucks RS, Hillman DR, Eastwood PR. Cognitive deficits in obstructive sleep apnea: Insights from a meta-review and comparison with deficits observed in COPD, insomnia, and sleep deprivation. Sleep Med Rev. 2018;38:39-49.

3. Azarbarzin A, Labarca G, Kwon Y, Wellman A. Physiologic Consequences of Upper Airway Obstruction in Sleep Apnea. Chest. 2024;166(5):1209-17.

4. Liu X, Ma Y, Ouyang R, Zeng Z, Zhan Z, Lu H, et al. The relationship between inflammation and neurocognitive dysfunction in obstructive sleep apnea syndrome. J Neuroinflammation. 2020;17(1):229.

5. Zhang X, Zhou H, Liu H, Xu P. Role of Oxidative Stress in the Occurrence and Development of Cognitive Dysfunction in Patients with Obstructive Sleep Apnea Syndrome. Mol Neurobiol. 2024;61(8):5083-101.

6. He Y, Dong N, Wang X, Lv RJ, Yu Q, Yue HM. Obstructive sleep apnea affects cognition: dual effects of intermittent hypoxia on neurons. Sleep Breath. 2024;28(3):1051-65.

7. Wen ZW, Liang DS, Cai XH, Chen J. The role of AMPK/mTOR signal pathway in brain injury following chronic intermittent hypoxia in growing rats. Eur Rev Med Pharmacol Sci. 2018;22(4):1071-7.
8. Wang G, Wang JJ, Chen XL, Du SM, Li DS, Pei ZJ, et al. The JAK2/STAT3 and mitochondrial pathways are essential for quercetin nanoliposome-induced C6 glioma cell death. Cell Death Dis. 2013;4(8):e746.
9. Jia T, Xing Z, Wang, Li G. Protective effect of dexmedetomidine on intestinal mucosal barrier function in rats after cardiopulmonary bypass. Exp Biol Med (Maywood). 2022;247(6):498-508.
10. Sun P, Xue Y. Silence of TANK-binding kinase 1 (TBK1) regulates extracellular matrix degradation of chondrocyte in osteoarthritis by janus kinase (JAK)-signal transducer of activators of transcription (STAT) signaling. Bioengineered. 2022;13(1):1872-9.
11. Philips RL, Wang Y, Cheon H, Kanno Y, Gadina M, Sartorelli V, et al. The JAK-STAT pathway at 30: Much learned, much more to do. Cell. 2022;185(21):3857-76.
12. Ballinger EC, Ananth M, Talmage DA, Role LW. Basal Forebrain Cholinergic Circuits and Signaling in Cognition and Cognitive Decline. Neuron. 2016;91(6):1199-218.
13. Lebois EP, Schroeder JP, Esparza TJ, Bridges TM, Lindsley CW, Conn PJ, et al. Disease-Modifying Effects of M(1) Muscarinic Acetylcholine Receptor Activation in an Alzheimer's Disease Mouse Model. ACS Chem Neurosci. 2017;8(6):1177-87.
14. Joshi YB, Thomas ML, Braff DL, Green MF, Gur RC, Gur RE, et al. Anticholinergic Medication Burden-Associated Cognitive Impairment in Schizophrenia. Am J Psychiatry. 2021;178(9):838-47.
15. Stožer A, Markovič R, Dolenšek J, Perc M, Marhl M, Slak Rupnik M, et al. Heterogeneity and Delayed Activation as Hallmarks of Self-Organization and Criticality in Excitable Tissue. Front Physiol. 2019;10:869.
16. Nicolas CS, Peineau S, Amici M, Csaba Z, Fafouri A, Javalet C, et al. The Jak/STAT pathway is involved in synaptic plasticity. Neuron. 2012;73(2):374-90.
17. Chiba T, Yamada M, Sasabe J, Terashita K, Shimoda M, Matsuoka M, et al. Amyloid-beta causes memory impairment by disturbing the JAK2/STAT3 axis in hippocampal neurons. Mol Psychiatry. 2009;14(2):206-22.
18. Qin Huang，Pei Wang HL, Mingjian Li,Yujiao Yue,Ping XU. Inhibition of ERK1/2 regulates cognitive function by decreasing expression levels of PSD-95 in the hippocampus of CIH rats. 2022.
19. Huang Q, Wang P, Liu HJ, Li MJ, Yue YJ, Xu P. Inhibition of ERK1/2 regulates cognitive function by decreasing expression levels of PSD-95 in the hippocampus of CIH rats. Eur J Neurosci. 2022;55(6):1471-82.
20. Verrall CE, Yang JYM, Chen J, Schembri A, d'Udekem Y, Zannino D, et al. Neurocognitive Dysfunction and Smaller Brain Volumes in Adolescents and Adults With a Fontan Circulation. Circulation. 2021;143(9):878-91.
21. Cerium Oxide Nanoparticles Promote Neurogenesis and Abrogate Hypoxia-Induced Memory Impairment through AMPK-PKC-CBP Signaling Cascade [Retraction]. Int J Nanomedicine. 2022;17:5163-4.
22. Morris RG, Garrud P, Rawlins JN, O'Keefe J. Place navigation impaired in rats with

hippocampal lesions. Nature. 1982;297(5868):681-3.
23. Tan YJ, Lee YT, Mancera RL, Oon CE. BZD9L1 sirtuin inhibitor: Identification of key molecular targets and their biological functions in HCT 116 colorectal cancer cells. Life Sci. 2021;284:119747.
24. Li C, Wang J, Wang Q, Zhang Y, Zhang N, Lu L, et al. Qishen granules inhibit myocardial inflammation injury through regulating arachidonic acid metabolism. Sci Rep. 2016;6:36949.
25. Caffarel MM, Zaragoza R, Pensa S, Li J, Green AR, Watson CJ. Constitutive activation of JAK2 in mammary epithelium elevates Stat5 signalling, promotes alveologenesis and resistance to cell death, and contributes to tumourigenesis. Cell Death Differ. 2012;19(3):511-22.
26. Xu D, Shen H, Tian M, Chen W, Zhang X. Cucurbitacin I inhibits the proliferation of pancreatic cancer through the JAK2/STAT3 signalling pathway in vivo and in vitro. J Cancer. 2022;13(7):2050-60.
27. La Sala G, Michiels C, Kükenshöner T, Brandstoetter T, Maurer B, Koide A, et al. Selective inhibition of STAT3 signaling using monobodies targeting the coiled-coil and N-terminal domains. Nat Commun. 2020;11(1):4115.
28. Bischof R, Gjevestad JGO, Ordiz A, Eldegard K, Milleret C. High frequency GPS bursts and path-level analysis reveal linear feature tracking by red foxes. Sci Rep. 2019;9(1):8849.
29. Mao Y, van Hoef V, Zhang X, Wennerberg E, Lorent J, Witt K, et al. IL-15 activates mTOR and primes stress-activated gene expression leading to prolonged antitumor capacity of NK cells. Blood. 2016;128(11):1475-89.
30. Wang M, Han X, Yu T, Wang M, Luo W, Zou C, et al. OTUD1 promotes pathological cardiac remodeling and heart failure by targeting STAT3 in cardiomyocytes. Theranostics. 2023;13(7):2263-80.
31. Qu HM, Qu LP, Li XY, Pan XZ. Overexpressed HO-1 is associated with reduced STAT3 activation in preeclampsia placenta and inhibits STAT3 phosphorylation in placental JEG-3 cells under hypoxia. Arch Med Sci. 2018;14(3):597-607.
32. Zhao H, Feng Y, Wei C, Li Y, Ma H, Wang X, et al. Colivelin Rescues Ischemic Neuron and Axons Involving JAK/STAT3 Signaling Pathway. Neuroscience. 2019;416:198-206.
33. Klein P, Dingledine R, Aronica E, Bernard C, Blümcke I, Boison D, et al. Commonalities in epileptogenic processes from different acute brain insults: Do they translate? Epilepsia. 2018;59(1):37-66.
34. Wang W, Hu W. Salvianolic acid B recovers cognitive deficits and angiogenesis in a cerebral small vessel disease rat model via the STAT3/VEGF signaling pathway. Mol Med Rep. 2018;17(2):3146-51.
35. Zhang ZA, Sun Y, Yuan Z, Wang L, Dong Q, Zhou Y, et al. Insight into the Effects of High-Altitude Hypoxic Exposure on Learning and Memory. Oxid Med Cell Longev. 2022;2022:4163188.
36. Park SJ, Shin EJ, Min SS, An J, Li Z, Hee Chung Y, et al. Inactivation of JAK2/STAT3 signaling axis and downregulation of M1 mAChR cause cognitive impairment in klotho mutant mice, a genetic model of aging. Neuropsychopharmacology. 2013;38(8):1426-37.
37. Mai HN, Sharma N, Shin EJ, Nguyen BT, Nguyen PT, Jeong JH, et al. Exposure to far-infrared rays attenuates methamphetamine-induced recognition memory impairment via modulation of the muscarinic M1 receptor, Nrf2, and PKC. Neurochem Int. 2018;116:63-76.

38. Galloway CR, Ravipati K, Singh S, Lebois EP, Cohen RM, Levey AI, et al. Hippocampal place cell dysfunction and the effects of muscarinic M(1) receptor agonism in a rat model of Alzheimer's disease. Hippocampus. 2018;28(8):568-85.
39. Mao LM, Young L, Chu XP, Wang JQ. Regulation of Src family kinases by muscarinic acetylcholine receptors in heterologous cells and neurons. Front Mol Neurosci. 2023;16:1340725.
40. Sumi T, Harada K. Muscarinic acetylcholine receptor-dependent and NMDA receptor-dependent LTP and LTD share the common AMPAR trafficking pathway. iScience. 2023;26(3):106133.
41. Zent KH, Dell'Acqua ML. Synapse-to-Nucleus ERK→CREB Transcriptional Signaling Requires Dendrite-to-Soma Ca(2+) Propagation Mediated by L-Type Voltage-Gated Ca(2+) Channels. J Neurosci. 2025;45(4).
42. Yohn SE, Harvey PD, Brannan SK, Horan WP. The potential of muscarinic M(1) and M(4) receptor activators for the treatment of cognitive impairment associated with schizophrenia. Front Psychiatry. 2024;15:1421554.
43. Nguyen HTM, van der Westhuizen ET, Langmead CJ, Tobin AB, Sexton PM, Christopoulos A, et al. Opportunities and challenges for the development of M(1) muscarinic receptor positive allosteric modulators in the treatment for neurocognitive deficits. Br J Pharmacol. 2024;181(14):2114-42.